Stanford Exploration Project, Report 73, November 18, 1997, pages 339–350

Stanford Exploration Project, Report 73, November 18, 1997, pages 339–350

Elastic modeling in discontinuous media: testing the dynamic response

Carlos A. Cunha Filho[1]

keywords: *modeling, amplitudes, elastic*

ABSTRACT

A simple discontinuous model with known analytical solution is used to compare the dynamic response of three elastic modeling schemes. One scheme is based on the Haskell-Thomson propagator-matrix and the other two are based on finite-differences. One of the finite-difference schemes follows the traditional discretization of the elastic wave equation while the other is based on a discretization approach developed for discontinuous media. Except for a higher dispersion in the traditional finite-differences, all approaches show a similar behavior at small angles of incidence. At larger illumination angles, the modified finite-difference and the propagator-matrix methods are much closer to the analytical solution than the traditional finite-difference approach. These results may have a considerable impact in the accuracy of finite-differences-based inversion schemes whenever the subsurface geology is better described (within the resolution wavelength of the data) by a model with sharp interfaces rather than by a smoothly varying model.

INTRODUCTION

Some important aspects of accurate finite-difference elastic modeling algorithms are the use of high-order differential operators, staggered grid computations, and a two-step implementation of the spatial operator by first obtaining the strains and then the stresses (Virieux, 1984, Dablain, 1986; Mora, 1986; Etgen, 1989). The high-order operators are required to avoid numerical anisotropy and dispersion, while the staggered scheme is important to allow the use of more accurate and stable operators, which have an even number of points, in a spatially synchronized way. One problem with these schemes is the lack of distinction between model and wavefield properties. The same differential operators are applied to the components of the wavefield and to the components of the stiffness tensor. This is appropriate for smooth models but not for blocky, discontinuous models, in which two-point operators are more suitable than larger operators for computing the derivatives of the elastic parameters of the model.

[1]**email:** not available

The method developed in Cunha (1991) observes this important distinction by completely decoupling the computation of stiffness derivatives from the computation of wavefield derivatives. I test here an improved version of this method which uses the equivalence relations defined in the algebra of Schoenberg and Muir (1989), and a modified version of the conventional staggered grid introduced in wave-equation modeling by Virieux (1984; 1986) to implement the discretization process. A complete description of this method, which is referred to as the *dual-operator method*, is given in Cunha (1992). This approach was efficiently implemented on a parallel platform and the resulting wavefields were compared with the analytical solution and with the results from other elastic modeling schemes. For the simple model tested the dual-operator method proved to be more accurate than the traditional finite-difference method, using operators of same order in time and space.

DYNAMIC BEHAVIOR

The kinematics of the wavefield are not affected by the introduction of a short operator to compute the model derivatives nor by using equivalent medium theory in the evaluation of the spatial operator. I introduced these changes to better simulate the dynamics of the wave-propagation problem. A simple model with horizontal layers was used to compare the dual-operator approach with a traditional finite-difference algorithm, and with an elastic modeling algorithm based on the Haskell-Thomson propagator-matrix method (Aki and Richards, 1980), which is restricted to horizontally-layered models. To test the stability and accuracy of these three schemes in extreme conditions, a water layer was placed at the top of the model.

Reflection seismograms from a simple model

Figure **??** describes the model parameters. Figure **??** shows the horizontal and vertical components of the wavefield generated by the dual-operator modeling scheme using the model of Figure **??**. The reflections with zero-offset traveltime equal to 0.8, 1.1, and 1.55 seconds correspond, respectively, to the water-bottom reflection, the reflection in the interface between the second and third layers, and the first multiple of the water-bottom reflection. The two other visible reflections correspond to the PS and SS reflections at the interface between the second and third layers.

Figure **??** shows the vertical and horizontal components of the wavefield generated with the Haskell-Thomson scheme, and Figure **??** shows the vertical and horizontal components of the wavefield generated with the traditional finite-difference scheme.

The wavelet is clearly broader in both finite-difference-based methods because they require that the source extends over more than one grid-point. That is also the reason for the small precursor lobe in the wavelet generated by these two methods. Although both finite-difference schemes have operators with the same number of points (of same order in time and space), the traditional method is more dispersive,

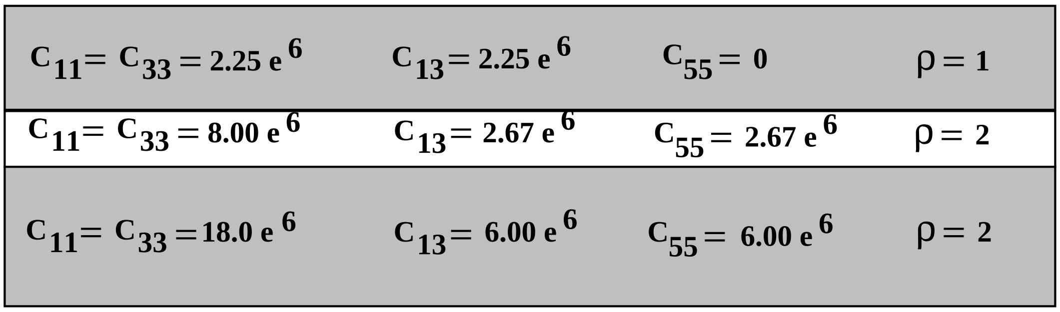

Figure 1: Model used to compare the results obtained with three different modeling schemes. Elastic constants are given in N/m^2, and densities in g/cm^3. carlos2-Mod.model [NR]

as indicated by the high-frequency ringing that contaminates the near traces of the vertical component. This higher dispersion is noticeable mainly when a liquid layer is present. Other differences are: the phase change of the sea bottom reflection near the offset 1300 meters in the vertical component of the traditional finite-difference scheme, the much weaker amplitude of the PSSP mode (the third event from the bottom) in the traditional finite-difference scheme, and the weaker near-offset amplitude of the PSPP mode (the fourth event from the bottom) in both finite-difference schemes relative to the propagator-matrix scheme.

The zero-offset waveform

The first comparison involves the zero-offset response of the three methods. A window that includes the first two primary reflections (both PP) was selected from the zero-offset trace of the vertical components for the three simulated wavefields. Figure **??** shows the three waveforms. Except for small differences in the amplitude and the precursor lobe, the waveforms generated by the propagator-matrix and dual-operator methods are very similar. The dispersion is minimal and the kinematics are in accordance with theoretical expectations. The dispersive character observed in the wavefield of the traditional finite-difference scheme becomes more clear in the selected window. As a result of the dispersion, the traveltime difference between the two reflections (using the central picks as the measuring criterion) is slightly larger than the theoretical value.

The theoretical ratio between the amplitudes of the two reflections is given by

$$\frac{\mathrm{Amp}_2}{\mathrm{Amp}_1} = \frac{R_2}{R_1}\,(1 - R_1^2)\,\left[\frac{t_1 v_1^2}{(t_2 - t_1)v_2^2 + t_1 v_1^2}\right]^{1/2},$$

where the first term is the ratio between the normal incidence reflection coefficients, the second term is the two-way transmission coefficient, and the third term is the 2D-divergence relative correction. The value obtained from the propagator-matrix

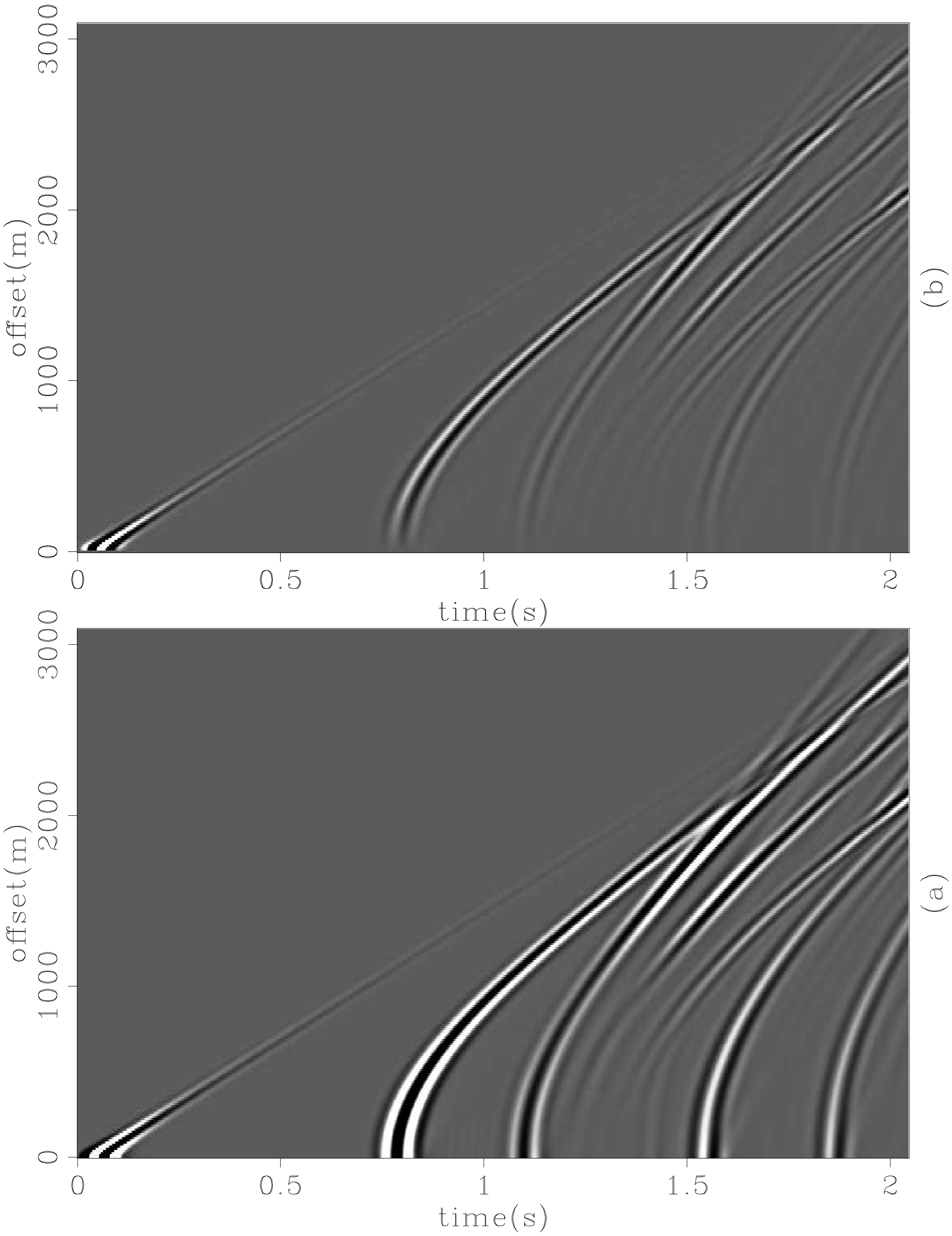

Figure 2: Surface wavefield generated by the dual-operator scheme. (a) Vertical component. (b) Horizontal component. carlos2-avoti [ER]

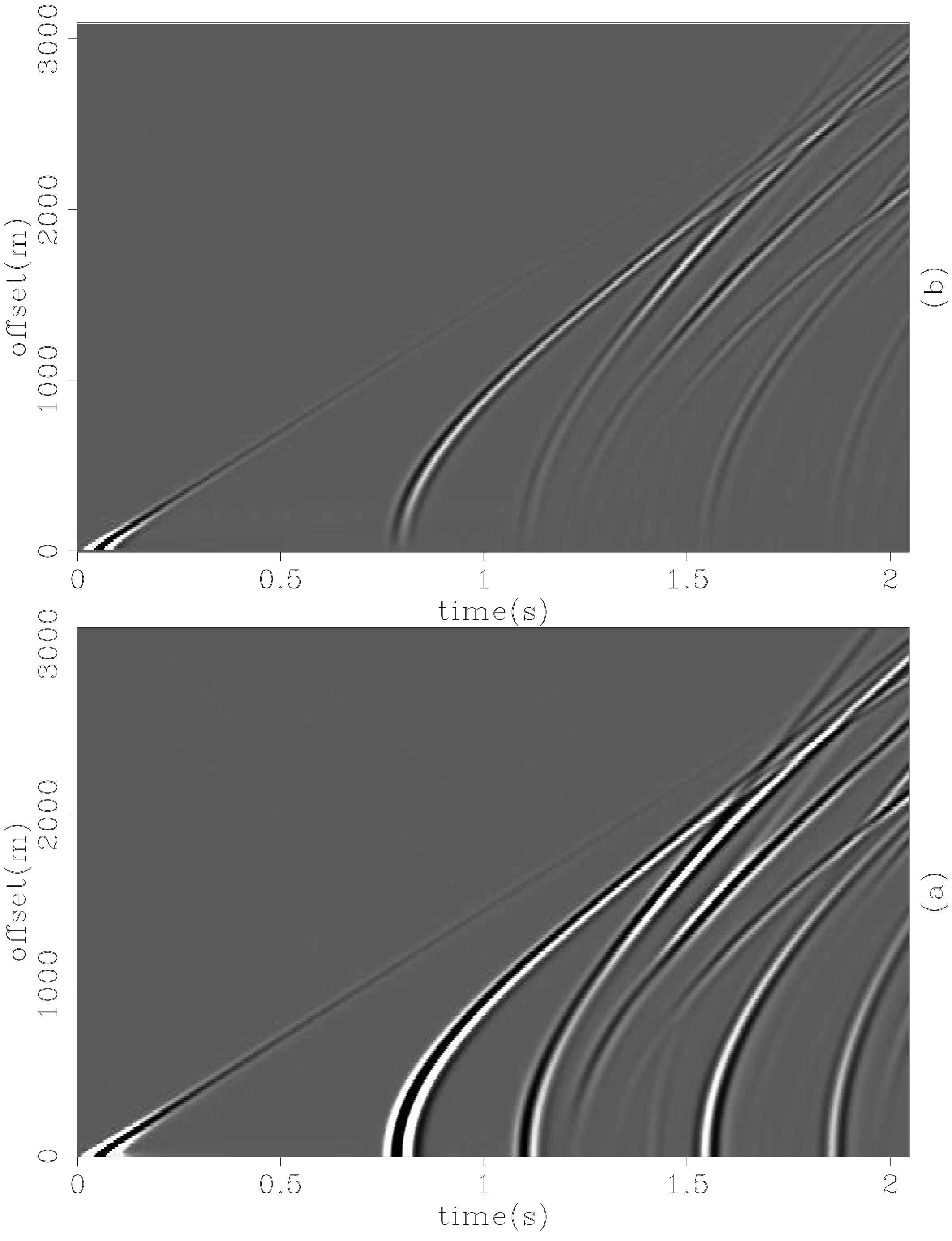

Figure 3: Surface wavefield generated by the propagator-matrix scheme. (a) Vertical component. (b) Horizontal component. carlos2-avosld [ER]

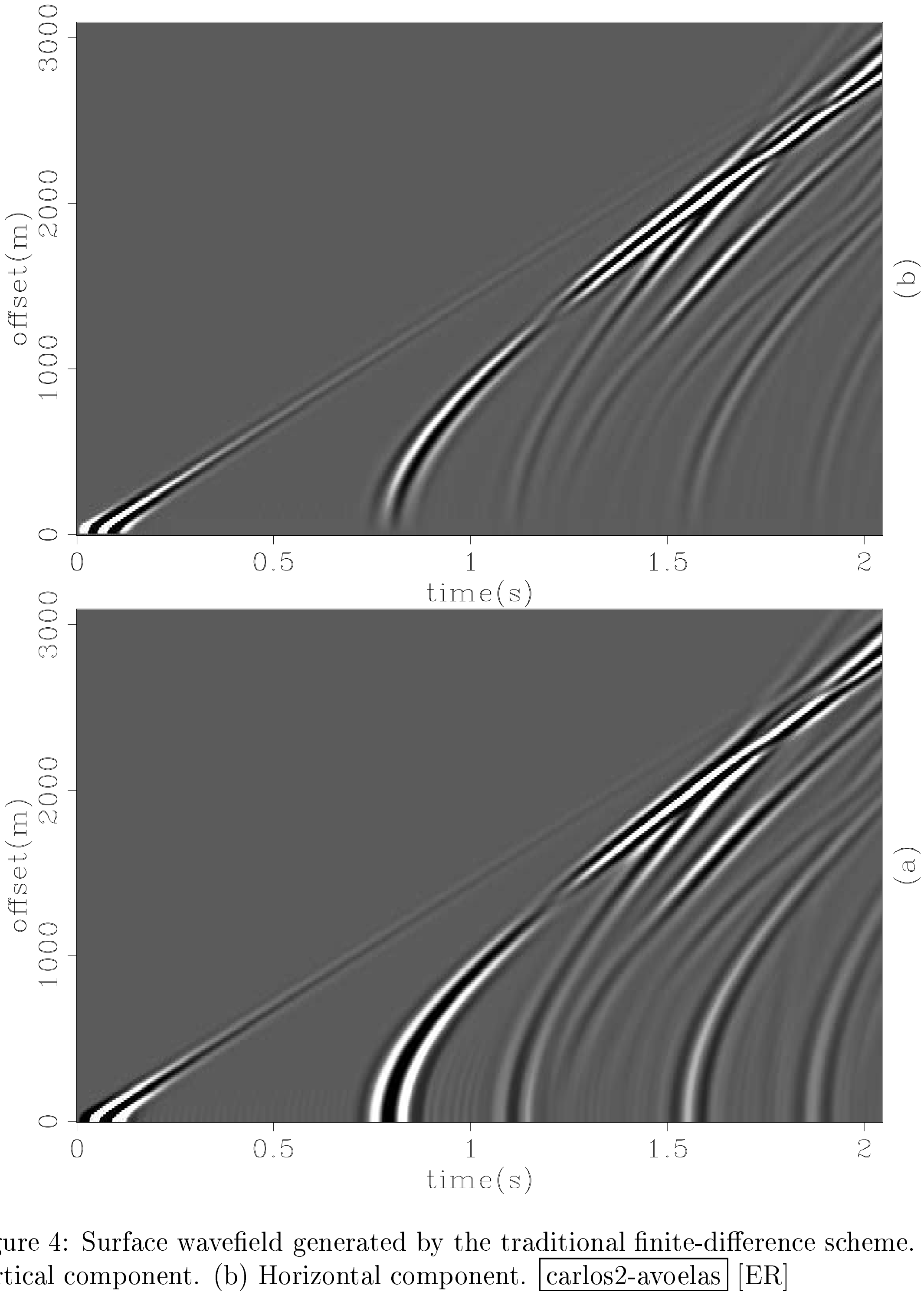

Figure 4: Surface wavefield generated by the traditional finite-difference scheme. (a) Vertical component. (b) Horizontal component. $\boxed{\text{carlos2-avoelas}}$ [ER]

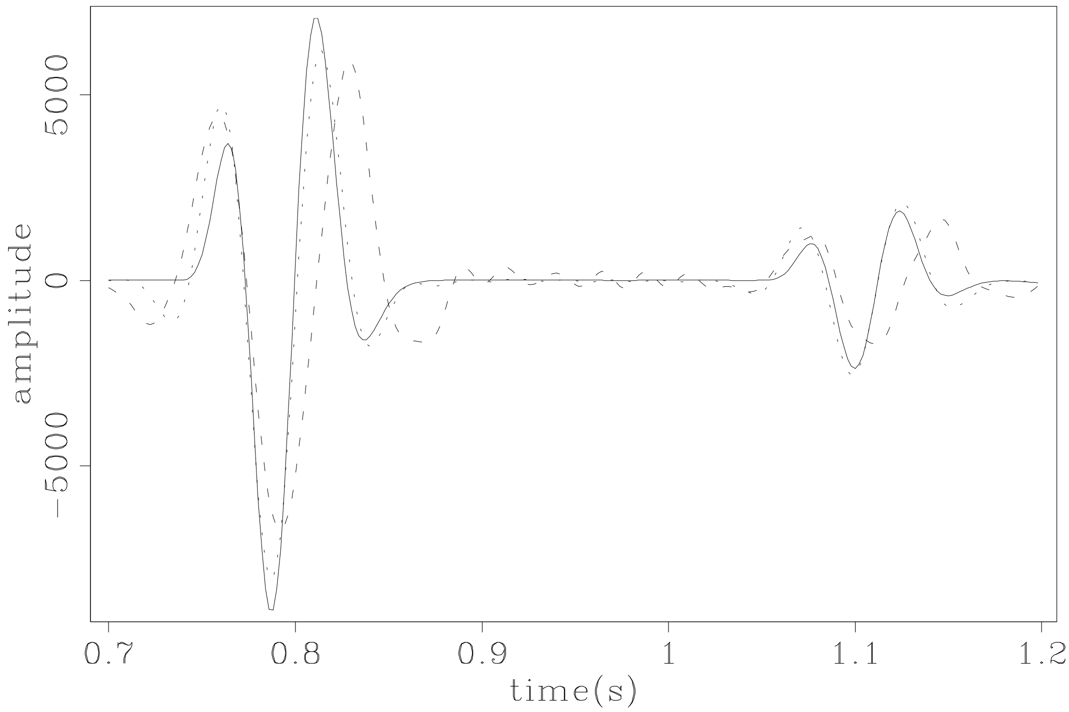

Figure 5: Zero offset response generated by the three schemes. The three curves correspond to a window selected from the first traces of Figures **??**-a, **??**-a, and **??**-a, which include the reflections from the first two interfaces of the model. The **continuous** line comes from the Haskell-Thomson scheme, the **dotted**-line comes from the dual-operator scheme, and the **dashed**-line comes from the traditional finite-difference scheme. carlos2-zeroresp [ER]

trace coincides with the predicted value, while the value from the dual-operator trace is 3.7 percent higher, and the value from the traditional finite-difference trace is 7.5 percent lower.

Amplitude versus offset

As important as the relative response between different reflections is the amplitude response of a single reflection as a function of the offset, or the illumination angle. The two P-to-P reflections of the previous subsection are separately analyzed here. To allow a direct comparison with the analytical curve for the PP plane-wave reflection coefficient, the wavefields simulated by each of the methods were mapped to the *tau–p* domain, which corresponds to the plane-wave decomposition of the original wavefields. Each figure used in this analysis contains five curves. The two continuous curves correspond to the real and imaginary parts of the theoretical P-to-P *plane-wave response* as a function of the horizontal slowness. The theoretical response includes the PP reflection coefficient and the two-way (angle-dependent) PP transmission coefficient. The other three curves come from the tau-p transform of the simulated wavefields, multiplied by a scaling factor that normalizes the amplitudes of the fifteenth horizontal slowness to the theoretical amplitude.

Figure **??** shows the curves associated with the water-bottom reflection. In the low horizontal slowness region the dual-operator curve (dashed-line) fits the theoretical curve almost perfectly, while the other two curves also represent a good approximation to the theoretical curve. It is also important to notice that the curve from the traditional finite-difference modeling (dashed-dotted-line) oscillates more than the other two curves. In the high horizontal slowness region, the traditional finite-difference method completely fails to approximate the theoretical curve while the other two methods still maintain a reasonably close fitting of the theoretical curve. One reason for the larger misfit here is the strong interference from the reflection of the second interface in the far offsets.

As in the previous case, the curves for the second PP primary reflection (Figure **??**) approximate well the theoretical curve for low values of horizontal slowness. Again, the curve from the traditional finite-difference scheme is much more jagged than the curves from the other two schemes. For larger values of horizontal slowness, the dual-operator and the propagator-matrix curves are closer to the theoretical curve than the traditional finite-difference curve with better fit than in the water bottom case, mainly because the interference from other events is much weaker in this case. Particularly impressive is the extremely good fit obtained by the dual-operator method (dashed-line) for the whole range[2] of horizontal slownesses, including the

[2]The apparent misfit observed at very small values of horizontal slowness is due to the absence of data from the other side of the source, which is particularly critical in a region where the events have large curvature. Notice that the amplitude values at vertical incidence are nearly half the theoretical value. Although the use of a split-spread recording geometry could have solved this problem, I decided to use a more realistic end-on geometry since the model corresponds to a marine

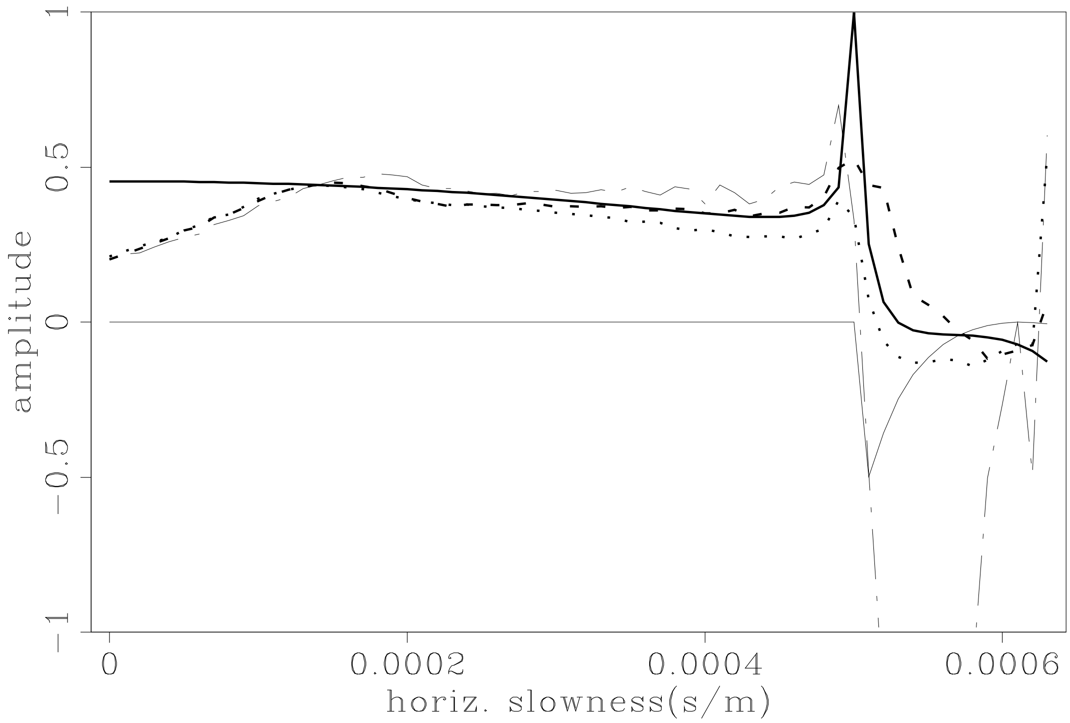

Figure 6: Amplitude versus horizontal slowness of the PP reflection from the water-bottom interface. These curves were extracted from the plane-wave decomposition of the wavefields generated by the three modeling schemes. The **thick continuous** line and the **thin continuous** line correspond, respectively, to the real and imaginary parts of the theoretical PP plane-wave reflection coefficient; the **dotted**-line is the amplitude response from the propagator-matrix scheme; the **dashed**-line is the amplitude response from the dual-operator scheme; the **thin dot-dashed**-line comes from the traditional finite-difference scheme. carlos2-avoresp1 [ER]

almost perfect prediction of the important zero-crossing point.

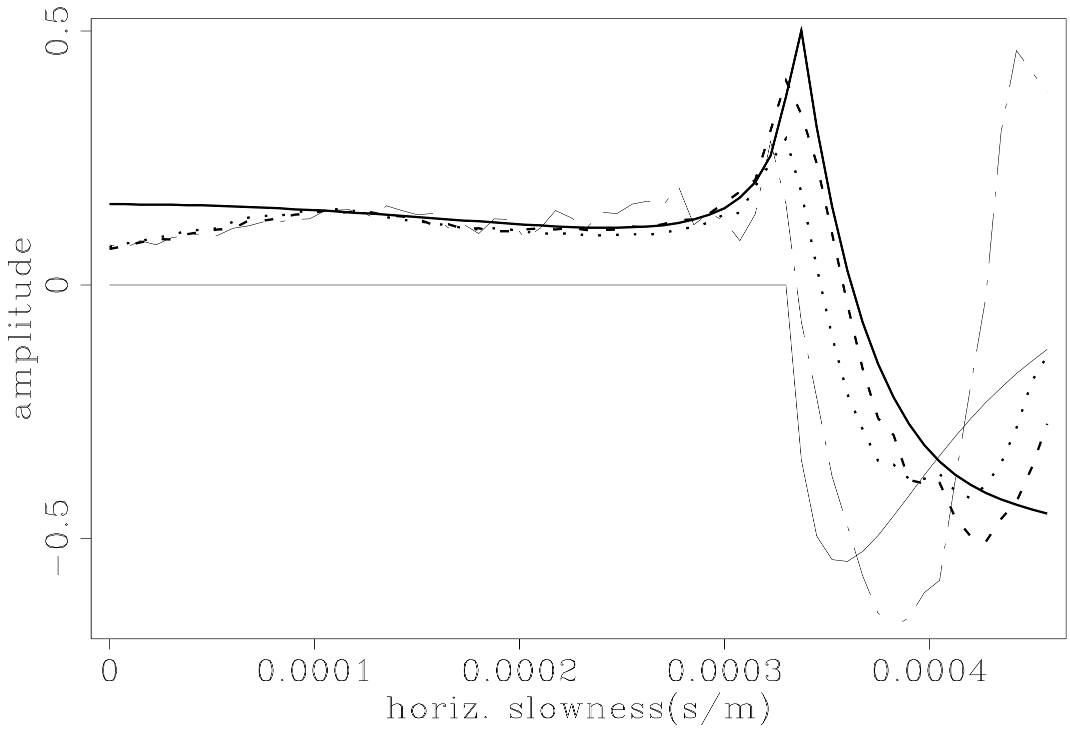

Figure 7: Amplitude versus horizontal slowness of the PP reflection from the interface between the second and third layer of the model. These curves were extracted from the plane-wave decomposition of the wavefields generated by the three modeling schemes. The **thick continuous** line and the **thin continuous** line correspond, respectively, to the real and imaginary parts of the theoretical PP plane-wave reflection coefficient; the **dotted**-line is the amplitude response from the propagator-matrix scheme; the **dashed**-line is the amplitude response from the dual-operator scheme; the **thin dot-dashed**-line comes from the traditional finite-difference scheme. $\boxed{\text{carlos2-avoresp2}}$ [ER]

SUMMARY

Traditional approaches to finite-difference elastic modeling make no distinction between model and wavefield variables. A single differential operator (either in the space or spatial-frequency domain) is used to calculate the spatial derivatives of both the stiffness components and the wavefield components. This lack of distinction can be in part attributed to the way in which most conventional schemes are implemented; the derivatives of the stiffness components are only implicitly computed when the derivatives of the stresses components are evaluated.

environment.

When the model parameters are a smooth function of the spatial variables, the same high-order, long operator can be used for both model and field derivatives, but when sharp boundaries are present, a short operator should be used for the derivatives of the model parameters. This approach, referred to as the dual-operator method, was implemented in a modified staggered grid within the framework of the equivalent media theory. For a simple model that includes a liquid layer the dual-operator method generated less dispersive more accurate results then the traditional finite-difference method. In particular, the angle-dependent plane-wave response obtained with the dual-operator method was more accurate than the one obtained with traditional finite-differences and at least as accurate as the one obtained with the propagator-matrix method.

ACKNOWLEDGMENTS

I would like to thank Jun Ji, Martin Karrembach and John Etgen for their constructive comments, suggestions and discussions.

REFERENCES

Aki, K., and Richards, P.G., 1980, Quantitative Seismology: Freeman and Company.

Cunha Filho, C.A., 1991, Modeling a discrete system by eigenvalue decomposition: SEP–**72**, 55–71.

Cunha Filho, C.A., 1992, Elastic inversion of marine data: Ph.D. thesis, Stanford University (in preparation).

Dablain, M.A., 1986, The application of high-order differencing to the scalar wave equation: Geophysics, **51**, 54–66.

Etgen, J.T., 1989, Accurate wave equation modeling: SEP–**60**, 131–147.

Mora, P., 1986, Elastic finite-differences with convolutional operators: SEP–**48**, 151–169.

Schoenberg, M., and Muir, F., 1989, A calculus for finely layered anisotropic media: Geophysics, **54**, 581–589.

Virieux, J., 1984, SH wave propagation in heterogeneous media: Velocity-stress finite-difference method: Geophysics, **49**, 1933–1937.

Virieux, J., 1986, P-SV wave propagation in heterogeneous media: Velocity-stress finite-difference method: Geophysics, **51**, 889–901.